ELSEVIER

Biochimica et Biophysica Acta 1553 (2002) 23–38

BIOCHIMICA ET BIOPHYSICA ACTA

BBA

www.bba-direct.com

Review

Fumarate respiration of *Wolinella succinogenes*: enzymology, energetics and coupling mechanism

Achim Kröger [a,*], Simone Biel [a], Jörg Simon [a], Roland Gross [a], Gottfried Unden [b], C. Roy D. Lancaster [c]

[a] *Institut für Mikrobiologie, Johann Wolfgang Goethe-Universität, Marie-Curie-Str. 9, D-60439 Frankfurt am Main, Germany*
[b] *Institut für Mikrobiologie und Weinforschung, Johannes Gutenberg-Universität, D-55099 Mainz, Germany*
[c] *Max-Planck-Institut für Biophysik, Heinrich-Hoffmann-Str. 7, D-60528 Frankfurt am Main, Germany*

Received 10 May 2001; received in revised form 27 August 2001; accepted 12 October 2001

Abstract

Wolinella succinogenes performs oxidative phosphorylation with fumarate instead of O_2 as terminal electron acceptor and H_2 or formate as electron donors. Fumarate reduction by these donors ('fumarate respiration') is catalyzed by an electron transport chain in the bacterial membrane, and is coupled to the generation of an electrochemical proton potential (Δp) across the bacterial membrane. The experimental evidence concerning the electron transport and its coupling to Δp generation is reviewed in this article. The electron transport chain consists of fumarate reductase, menaquinone (MK) and either hydrogenase or formate dehydrogenase. Measurements indicate that the Δp is generated exclusively by MK reduction with H_2 or formate; MKH_2 oxidation by fumarate appears to be an electroneutral process. However, evidence derived from the crystal structure of fumarate reductase suggests an electrogenic mechanism for the latter process.

Keywords: Fumarate respiration; Electron transport; Coupling mechanism; Hydrogenase; Formate dehydrogenase; *Wolinella succinogenes*

1. Introduction

The terms 'respiration' or 'aerobic respiration' refer to certain redox reactions with O_2 as acceptor that are catalyzed by membrane-integrated electron transport chains. These reactions are coupled to the generation of an electrochemical proton potential (Δp) across the membrane [1]. Many bacteria perform respiration with terminal electron acceptors such as fumarate, nitrate, polysulfide ([S]) or various

Abbreviations: DCPIP, 2,6-dichlorophenolindophenol; DMN, 2,3-dimethyl-1,4-naphthoquinone; $DMNH_2$, hydroquinone of DMN; HQNO, 2-*n*-heptyl-4-hydroxyquinoline-*N*-oxide; MD, 2-methyl-1,4-naphthoquinone; MDH_2, hydroquinone of MD; MK, menaquinone; MKH_2, hydroquinone of MK; NQ, 1,4-naphthoquinone; NQH_2, hydroquinone of NQ; NQNO, 2-*n*-nonyl-4-hydroxyquinoline-*N*-oxide; PMS, *N*-methylphenazinium sulfate; Q_O, 2,3-dimethoxy-5-methyl-1,4-benzoquinone; Q_OH_2, hydroquinone of Q_O; [S], polysulfide; vitamin K_1 (phylloquinone), 2-methyl-3-phytyl-1,4-naphthoquinone; Y^{max}, growth yield extrapolated to ∞ growth rate (g cells/mol substrate); Y^{max}_{ATP}, theoretical maximum growth yield (g cells/mol ATP); Δp, electrochemical proton potential (proton motive force) across a membrane (V); $\Delta\psi$, electrical proton potential across a membrane (V)

* Corresponding author. Fax: +49-69798-29527. *E-mail address:* a.kroeger@em.uni-frankfurt.de (A. Kröger).

0005-2728/02/$ – see front matter
PII: S0005-2728(01)00234-1

other compounds instead of O_2 [2–4]. These processes are termed 'anaerobic respiration'. Anaerobic respiration with fumarate is called 'fumarate respiration'. As in aerobic oxidative phosphorylation, the Δp generated by anaerobic respiration drives ATP synthesis from ADP and phosphate, catalyzed by ATP synthase. The ATP synthases involved in aerobic and anaerobic oxidative phosphorylation appear to operate according to similar mechanisms.

Depending on the bacterial species and on the metabolic situation, bacteria perform respiration with a wide variety of redox reactions. As a consequence, the composition of the respiratory chains and the mechanisms of Δp generation may vary greatly in aerobic and in anaerobic respiration. The coupling mechanisms of electron transport to apparent proton translocation are not known in most instances and are still under debate in the few most thoroughly studied cases of aerobic respiration [1,5,6]. A fundamental prerequisite for understanding coupling mechanisms has been provided in the last decade by the determination of the crystal structures of several electron transport enzymes [5–9].

In this contribution, the results of the biochemical investigation of fumarate respiration of *Wolinella succinogenes* will be discussed, taking into consideration recent evidence from the crystal structure of the fumarate reductase of this anaerobic bacterium. *W. succinogenes* fumarate respiration is the most extensively studied anaerobic respiration known today; it comprises two membrane-integrated enzymes (hydrogenase and formate dehydrogenase) in addition to fumarate reductase. Review articles on the structure and function of fumarate reductases and the related succinate dehydrogenases are included in this volume. The structural aspects of *W. succinogenes* fumarate reductase are reviewed by Lancaster and Simon in this volume. Comprehensive reviews on related topics were published earlier [2,9–14].

2. Composition of the fumarate respiratory chains

W. succinogenes can grow by fumarate respiration with either H_2 (Reaction a), formate (Reaction b) or sulfide (Reaction c) as electron donor [14]:

$$H_2 + \text{fumarate} \rightarrow \text{succinate} \quad \text{(a)}$$

$$HCO_2^- + \text{fumarate} + H_2O \rightarrow HCO_3^- + \text{succinate} \quad \text{(b)}$$

$$HS^- + \text{fumarate} + H^+ \rightarrow [S] + \text{succinate} \quad \text{(c)}$$

Reactions a–c are catalyzed by electron transport chains which are integrated in the membrane [12,15].

The electron transport chains catalyzing Reaction a or Reaction b consist of fumarate reductase, menaquinone (MK), and hydrogenase or formate dehydrogenase, respectively (Fig. 1). The enzymes have been isolated and the sequences of the corresponding genes have been determined (Sections 3–5). The crystal structure of fumarate reductase has been determined [8]. The composition of the electron transport chains has been confirmed by their reconstitution in liposomes from the isolated enzymes (Section 6).

Each of the three enzymes consists of one hydrophobic and two hydrophilic subunits. The larger of the hydrophilic subunits contain the catalytic sites, and the smaller are iron–sulfur proteins which serve in transferring electrons from the catalytic to the hydrophobic subunits or vice versa. The hydrophobic subunits are di-heme cytochromes *b* which react with MK or MKH_2 and anchor the enzymes in the membrane. The sequences of the cytochrome *b* subunits of hydrogenase and formate dehydrogenase are similar, and suggest that the four heme ligands are located on three membrane helices [16]. One of the heme groups is predicted to be closer to the periplasmic and the other closer to the cytoplasmic surface of the membrane. The catalytic subunit of

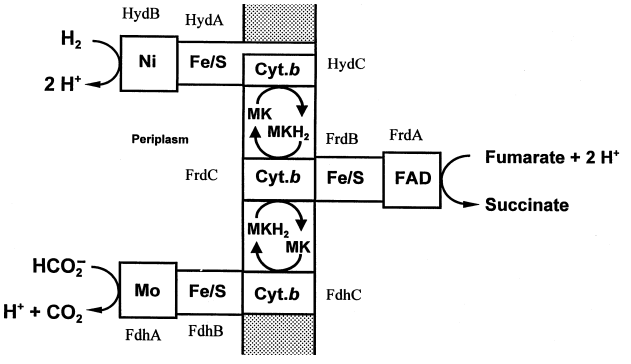

Fig. 1. The electron transport system of *W. succinogenes* catalysing fumarate respiration with H_2 (Reaction a) or formate (Reaction b), and the orientation of hydrogenase (Hyd), formate dehydrogenase (Fdh), and fumarate reductase (Frd).

hydrogenase is exposed to the periplasmic side of the membrane [17]. The catalytic site of formate dehydrogenase is also oriented to the periplasm, whereas that of fumarate reductase faces the cytoplasm [18].

The electron transport chain catalysing Reaction c, consists of fumarate reductase, and probably MK and sulfide dehydrogenase. The fumarate reductase involved in sulfide oxidation is identical to that in the electron transport chain catalysing Reaction b [19]. A mutant of *W. succinogenes* lacking the genes encoding the subunits of fumarate reductase did not grow by fumarate respiration with formate or with sulfide. The sulfide dehydrogenase has not yet been isolated and the genes have not yet been cloned.

3. Hydrogenase

A mutant of *W. succinogenes* lacking the genes encoding the subunits of hydrogenase did not grow at the expense of Reaction a [17]. When grown with formate and fumarate (Reaction b) the mutant did not contain hydrogenase activity, in contrast to the wild-type strain. Hydrogenase catalyzes the reduction by H_2 of the MK present in the membrane of *W. succinogenes* (Fig. 1). The site of MK reduction is located on the cytochrome *b* subunit (HydC). This is suggested by the finding that the isolated enzyme containing HydC catalyzed the reduction of the water-soluble MK-analogue DMN by H_2, whereas a preparation lacking HydC did not [20]. Both forms of the enzyme catalyzed viologen reduction by H_2. Furthermore, mutants of *W. succinogenes* with one of the four histidyl ligands of the heme groups of HydC replaced by other residues, catalyzed H_2 oxidation by viologen dyes, but not by DMN or fumarate [21]. The mutant enzymes were still bound to the membrane, and the membrane contained HydC, as shown by enzyme-linked immunosorbent assay. Hence an intact HydC subunit is required for quinone reduction by H_2.

Hydrogenase is anchored in the membrane by HydC and by the hydrophobic C-terminus of HydA [17]. Mutants lacking one of the anchors still had their hydrogenase bound to the membrane. In the absence of both anchors, HydB and the activity of viologen reduction by H_2 were located in the periplasm. A mutant lacking the C-terminus of HydA as well as a mutant with the conserved residue H305 in the C-terminus replaced by methionine had no activity of quinone reduction by H_2 [21]. The loss of quinone reactivity was probably not due to the loss of a heme group, since isolated HydC was found to carry the two heme groups (R. Gross and C.R.D. Lancaster, unpublished results). The mutations in *hydA* may possibly block electron transfer from HydA to HydC.

The two hydrophilic subunits HydA and HydB are similar to the two polypeptides making up the periplasmic Ni-hydrogenases of two *Desulfovibrio* species; the crystal structures of these enzymes are known [22,23]. The larger catalytic subunits (HydB) carry the Ni/Fe catalytic center and the smaller carry three iron–sulfur centers. The structures suggest that H_2 is split into electrons and protons at the catalytic center. The protons are released on the surface of HydB through a proton pathway, while the electrons are guided by the three consecutive iron–sulfur centers to the binding site of the electron acceptor on the surface of HydA. Since nearly all the relevant residues are also conserved in the hydrogenase of *W. succinogenes* and in other membrane-bound Ni-hydrogenases, it is likely that the catalytic mechanism also applies here.

4. Formate dehydrogenase

Two gene loci code for the subunits of the enzyme in *W. succinogenes* [24]. The two *fdh* operons differ in their promotor regions, but are nearly identical in their gene sequences. Deletion mutants lacking one of the operons still grow with formate as electron donor. The formate dehydrogenases of the mutants appear to be identical. The genes *fdhA*, *fdhB* and *fdhC* of the formate dehydrogenase operons *fdhEABCD* encode the subunits of the enzyme [25]. The functions of *fdhE* and *fdhD* are not known. The *fdhD* gene of *Escherichia coli* was shown to be required for the formation of an enzymically active formate dehydrogenase [26]. The proteins predicted by *fdhD* in the two organisms share 30% identity.

Formate dehydrogenase catalyzes the reduction of MK by formate (Fig. 1) [25,27,28]. The enzyme was isolated in two forms, FdhABC and FdhAB, one

containing and the other lacking cytochrome *b*. Both forms catalyzed the reduction of DMN by formate and could be incorporated into the membrane of liposomes [28]. However, restoration of the electron transport activity with formate and fumarate (Reaction b) in liposomes harboring vitamin K_1 and fumarate reductase also, was attained only with the preparation containing cytochrome *b*. These results suggest that the reaction site of lipophilic quinones such as MK or vitamin K_1 is located on the cytochrome *b* subunit (FdhC) of formate dehydrogenase, whereas the more hydrophilic DMN may also react at a second site.

The catalytic subunit FdhA contains molybdenum coordinated by molybdopterin guanine dinucleotide and is predicted to carry a [4Fe–4S] iron–sulfur center [25,29]. FdhB is predicted to carry four [4Fe–4S] or one [3Fe–4S] and three [4Fe–4S] iron–sulfur centers. The sequence of FdhA is similar to those of several other molybdo-oxidoreductases whose crystal structures are known, including formate dehydrogenase H of *E. coli* [30]. These enzymes share a deep crevice extending from the surface to the molybdenum, the site of substrate conversion. In *E. coli* formate dehydrogenase H, an iron–sulfur center is localized at an appropriate distance for rapid electron transfer from the molybdenum site. This suggests that formate is split at the molybdenum site to yield two electrons, CO_2 and a proton. While the electrons are transferred to the iron–sulfur center, CO_2 and the proton probably leave the catalytic site via the substrate crevice.

5. Fumarate reductase

W. succinogenes can form only one enzyme catalysing fumarate reduction to succinate [19]. A mutant lacking the genes encoding the subunits of the enzyme did not grow with formate and fumarate. When grown with formate and nitrate, the mutant did not contain fumarate reductase activity and did not catalyze electron transport from formate to fumarate, in contrast to the wild-type strain.

5.1. Catalytic properties

Fumarate reductase catalyzes the reduction of fumarate by MKH_2 which is present in the membrane of *W. succinogenes* (Fig. 1). The enzyme was isolated in two forms, one containing and the other lacking cytochrome *b* (FrdC) [31,32]. The enzyme containing cytochrome *b* catalyzed $DMNH_2$ oxidation by fumarate, whereas the other form did not. Both forms catalyzed fumarate reduction by benzyl viologen radical. Hence the site of the quinol reaction appears to be located on the cytochrome *b* subunit. In redox titration, half of the heme in the enzyme responded with a midpoint potential of −20 mV, whereas that of the other half was at −200 mV, relative to the standard hydrogen electrode.

The isolated fumarate reductase catalyzes the reduction of fumarate by $DMNH_2$ or MDH_2 as well as the oxidation of succinate by various quinones (Table 1). The activity of succinate oxidation by 1,4-naphthoquinone (NQ) or 2,3-dimethoxy-5-methyl-

Table 1
Reactivity of *W. succinogenes* fumarate reductase and of *B. subtilis* succinate dehydrogenase with hydrophilic quinones (quinols) [33]

Donor → acceptor	E'_o (mV)	$\Delta E'_o$ (mV)	Fumarate reductase (s^{-1})	Succinate dehydrogenase (s^{-1})
$DMNH_2$ → fumarate	−80	−110	103	58
MDH_2 → fumarate	−1	−31	46	36
NQH_2 → fumarate	+64	+34	≤1	2
Q_OH_2 → fumarate	+162	+132	≤1	≤1
Succinate → DMN	−80	+110	8.4	3.6
Succinate → MD	−1	+31	33	9.2
Succinate → NQ	+64	−34	50	36
Succinate → Q_O	+162	−132	47	26
Succinate → PMS/DCPIP	–	–	125	125

The activities refer to the enzymes as isolated, and are given as succinate turnovers per FAD. The FAD contents were 3.9 (succinate dehydrogenase) and 6.0 μmol/g protein (fumarate reductase). E'_o refers to the quinone/quinol couple. $\Delta E'_o$ designates the difference relative to $E'_o = +30$ mV of the fumarate/succinate couple.

1,4-benzoquinone (Q_O) is half that of fumarate reduction by $DMNH_2$. The activities appear to be determined mainly by the redox potentials of the quinone/quinol rather than by their structures. Thus in succinate oxidation, Q_O, a benzoquinone, is as effective an electron acceptor as is NQ, a naphthoquinone. Succinate dehydrogenase isolated from *Bacillus subtilis* catalyzes fumarate reduction by $DMNH_2$ with a higher activity than succinate oxidation by any of the quinones. This enzyme is as active as fumarate reductase in succinate oxidation by *N*-methylphenazinium sulfate (PMS)/2,6-dichlorophenolindophenol (DCPIP). The activities of fumarate reduction with the quinols as well as those of succinate oxidation by the quinones of the *B. subtilis* enzyme do not differ significantly from those of fumarate reductase.

The reactivity with lipophilic quinones was investigated after incorporation of each of the two enzymes into liposomes which contained either ubiquinone-9 or vitamin K_1 [33]. The activity of succinate oxidation of both enzymes was five times higher with ubiquinone-9 than with vitamin K_1, although *W. succinogenes* and *B. subtilis* only contain MK, a naphthoquinone, like vitamin K_1. In summary, *W. succinogenes* fumarate reductase and *B. subtilis* succinate dehydrogenase catalyze fumarate reduction as well as succinate oxidation with commensurate activities. Their reactivity is not restricted to naphthoquinones.

5.2. Kinetic response of the prosthetic groups

The crystal structure of fumarate reductase indicates that the prosthetic groups are lined up to form an unbranched electron pathway from the distal heme group of the cytochrome *b* subunit (FrdC) to FAD in the catalytic subunit FrdA (Figs. 2 and 3) [8]. The three iron–sulfur centers are bound to FrdB with the [2Fe–2S] center close to FAD, the [3Fe–4S] center close to the proximal heme group, and the [4Fe–4S] center in between. The velocity of reduction of cytochrome *b*, and of the [3Fe–4S] and the [2Fe–2S] iron–sulfur centers was measured upon the addition of $DMNH_2$ to the fully oxidized enzyme (Fig. 2A) [34]. The apparent first order reduction rates of the three prosthetic groups were slightly higher than the turnover number of the enzyme catalysing fumarate reduction by $DMNH_2$ (133 s^{-1}). This result is consistent with the view that the reduction rate of each prosthetic group is limited by the velocity of $DMNH_2$ oxidation at the cytochrome *b* subunit. It should be mentioned that only half of the two heme groups is reduced by $DMNH_2$. Reduction of the other half is achieved by dithionite or viologen radicals.

Measurement of the velocity of oxidation of the three prosthetic groups in the fully reduced enzyme upon the addition of fumarate gave a surprising result which is not yet understood (Fig. 2B). The two heme groups are oxidized in an apparently homoge-

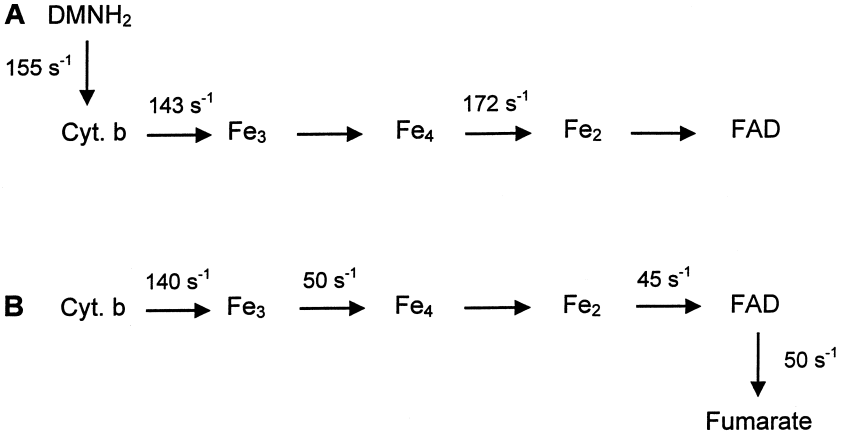

Fig. 2. Arrangement of the prosthetic groups of fumarate reductase relative to the sites of $DMNH_2$ oxidation (A) and of fumarate reduction (B) [8]. The rate constants refer to the reduction of the components in the fully oxidized enzyme upon the addition of $DMNH_2$ (A), and to their oxidation in the fully reduced enzyme by fumarate (B) at 20°C [34]. The turnover number in fumarate reduction by $DMNH_2$ based on the FAD content of the enzyme was 133e s^{-1} at 20°C. Fe_2, Fe_3, and Fe_4 designate the [2Fe–2S], the [3Fe–4S], and the [4Fe–4S] iron–sulfur center, respectively.

neous first order reaction with a rate constant close to the turnover number of fumarate reduction by $DMNH_2$. In contrast, the rate of oxidation of the [2Fe–2S] center, and that of the appearance of the flavin radical, was less than half the enzymatic turnover number. The [3Fe–4S] center was oxidized in two phases. Half of the center responded approximately as fast as the [2Fe–2S] center (Fig. 2B), whereas the other half reacted about 10 times slower (not shown).

5.3. Function of the subunits

To investigate the function of the individual subunits, fumarate reductase was split with guanidinium to yield FrdA, FrdB, FrdC, and FrdAB (Fig. 1) [32]. FrdA and FrdAB catalyzed fumarate reduction by benzyl viologen and succinate oxidation by methylene blue, but did not react with $DMNH_2$. Restoration of the activity of fumarate reduction by $DMNH_2$ was achieved by coprecipitation with polyethylene glycol of FrdA with FrdB and FrdC or of FrdAB with FrdC. FrdC contained 0.4 mol heme per mol, 85% of which was of the high-potential type ($E_m = -15$ mV) and was reduced upon $DMNH_2$ addition. The residual heme (15%) was of the low-potential type ($E_m = -150$ mV). The difference spectrum (reduced−oxidized) of the isolated FrdC was nearly identical to that observed with the intact enzyme upon reduction with $DMNH_2$.

The activity of fumarate reduction by $DMNH_2$ restored from coprecipitated FrdAB and FrdC was a function of the amount of FrdC; saturation was reached with approximately 3 mol FrdC per mol FrdAB. With equimolar amounts of FrdAB and FrdC, 40% of the maximal activity was measured. This suggests that an equimolar amount of FrdC containing the high-potential heme group is bound to FrdAB in the reconstituted enzyme which can catalyze fumarate reduction by $DMNH_2$.

Preparations of FrdA and FrdAB containing various amounts of FrdB were reconstituted using a fivefold molar amount of FrdC. The amount of heme reduced by succinate in the resulting preparation was equimolar to that of the FrdB present, suggesting that FrdC is bound to FrdB and that the heme group of the bound FrdC is accessible to the electrons provided by succinate oxidation. The simplest interpretation of these results is that the proximal heme group (b_P) is the high-potential one and that this heme group is present in the isolated FrdC (Fig. 3). The site of $DMNH_2$ oxidation should be located within electron transfer distance (< 14 Å) [35] to the proximal heme. The distal low-potential heme group (b_D) is apparently not required for the electron transfer from $DMNH_2$ to fumarate, although it is reduced by H_2 or formate in the bacterial membrane, and the reduced heme group is oxidized by fumarate at the rate of fumarate reductase activity with $DMNH_2$ (Fig. 2B). The interpretation is based on the assumption that the site of $DMNH_2$ oxidation on FrdC is the same in the reconstituted and in the original enzyme, in spite of the removal of the distal heme group.

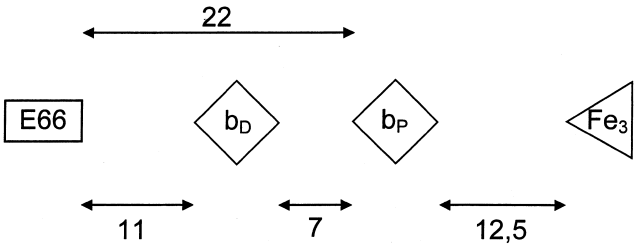

Fig. 3. Distances (in Å) between prosthetic groups of fumarate reductase [8]. The distal (b_D) and the proximal (b_P) heme groups are located in FrdC (Fig. 1). Residue E-66 is close to the periplasmic membrane surface. The [3Fe–4S] iron–sulfur cluster (Fe_3) is located on the cytoplasmic side of the membrane.

6. The function of MK and reconstitution of the electron transport chains

MK is present in the membrane of *W. succinogenes* in approximately 10-fold and 100-fold the molar amount of fumarate reductase and of formate dehydrogenase, respectively [36,37]. Nearly all the MK present in the membrane fraction is reduced to MKH_2 by formate. MKH_2 is reoxidized upon addition of fumarate. In the steady state of electron transport from formate to fumarate, the redox state of MK depends on the activities of formate dehydrogenase and of fumarate reductase. The redox state is increasingly oxidized upon progressive inhibition of formate dehydrogenase and is increasingly reduced upon increasing inhibition of fumarate reductase.

This response is typical of a respiratory component and suggests that nearly all the MK present in the membrane participates in the electron transport.

MK is an obligatory constituent of the electron transport chains catalysing fumarate respiration with H_2 or formate. This is indicated by the loss of electron transport activity with formate upon extraction of MK from the bacterial membrane fraction and by the restoration of the activity after reincorporation of MK [36]. Furthermore, the electron transport activity with H_2 or formate of liposomes containing fumarate reductase and either hydrogenase or formate dehydrogenase was shown to be dependent on the presence of MK or vitamin K_1 [27,38,39].

The reconstitution in liposomes of the functional electron transport chains catalysing fumarate reduction by H_2 or formate indicates that the isolated enzymes contain all the constituents required for electron transport. The activity of fumarate reduction by formate in the liposomes was as sensitive to 2-*n*-nonyl-4-hydroxyquinoline-*N*-oxide (NQNO) as that in the bacterial membrane, suggesting the same pathway of the electrons in both preparations [27]. NQNO (like 2-*n*-heptyl-4-hydroxyquinoline-*N*-oxide, HQNO) inhibits the electron transfer from formate dehydrogenase to MK in *W. succinogenes* and is probably bound to the cytochrome *b* subunit (FdhC) of the enzyme [40].

The specific activity of DMN reduction by formate of the formate dehydrogenase in the proteoliposomes was 15% of that of the enzyme in the bacterial membrane, while 70% of the fumarate reductase activity with $DMNH_2$ was obtained after isolation and incorporation [27,37]. The loss of formate dehydrogenase activity was mainly due to the isolation procedure which caused partial dissociation of FdhC from the enzyme. Approximately 80% of the enzyme molecules were found on the outer surface of the liposomes and were, therefore, accessible to their substrates. The activities of the two enzymes (V_{Fdh} and V_{Frd}) were related to the overall electron transport activity (V_{ET}) according to Eq. 1:

$$V_{ET} = V_{Fdh}V_{Frd}/(V_{Fdh} + V_{Frd}) \quad (1)$$

Eq. 1 refers to a system of two consecutive enzymes with a common intermediate (quinol) which is formed by the first enzyme and used by the second. As predicted by Eq. 1, the electron transport activity in the liposomes was half that of the individual enzymes, when their activities were the same. When one enzyme activity was in large excess, the electron transport activity was close to the activity of the limiting enzyme. This result shows that all the active enzyme molecules participate in the electron transport, independent of their contents in the proteoliposomes. This is due to the 'pool function' of lipophilic quinones in the membrane which allows every quinone molecule to be reduced by each dehydrogenase molecule, and to transfer electrons to each fumarate reductase molecule.

7. Energetics of fumarate respiration

The ATP synthase isolated from *W. succinogenes* was shown to catalyze ATP synthesis from ADP and inorganic phosphate at the expense of an artificial Δp, after the enzyme had been incorporated into the membrane of liposomes [41]. At a sufficiently high Δp, the turnover number of the enzyme in ATP synthesis was commensurate to that in the growing bacteria. From the velocity of ATP synthesis and the corresponding H^+ flux across the membrane of the liposomes the amount of H^+ translocated per ATP synthesized (H^+/ATP ratio) was estimated to be 3 [42].

Cells of *W. succinogenes* catalysing fumarate respiration with formate were found to contain nearly equal amounts of ATP and ADP [43]. Assuming the cellular concentration of free phosphate to be 1 and 10 mM, the cellular phosphorylation potential at pH 7 ($\Delta G'_P$) is calculated from the standard potential ($\Delta G'_o = 32$ kJ/mol ATP) to be 50 and 44 kJ/mol ATP, respectively.

Since fumarate reductase is oriented towards the cytoplasm, fumarate and succinate are transported across the membrane during fumarate respiration (see review by Janausch et al. in this volume). In the presence of Na^+, the two di-carboxylates are transported simultaneously according to an electroneutral antiport mechanism [60]. Therefore, the ATP/e and the H^+/e ratios measured with cells should not be impaired by the dicarboxylate transport, provided that the cells contain succinate and Na^+ is present.

7.1. Theoretical ATP/e and H^+/e ratios

The ATP/e ratio designates the amount of ATP formed from ADP and inorganic phosphate per mol electrons transported from the donor (e.g. H_2 or formate) to the acceptor substrate (e.g. fumarate). The H^+/e ratio designates the amount of protons apparently translocated across the membrane per mol electrons transported from the donor to the acceptor substrate.

The theoretical maximum ATP/e ratio, $(n_{ATP}/n_e)_{max}$, is calculated from the $\Delta G'_P$ and the $\Delta E'_o$ of fumarate reduction by H_2 or formate, according to Eq. 2 where F represents the Faraday constant:

$$(n_{ATP}/n_e)_{max} = \Delta E'_o F/\Delta G'_P \quad (2)$$

With $\Delta G'_P = 50$ kJ/mol ATP, the maximum ATP/e ratio is obtained as 0.87 (Table 2). Using this value, and the number of protons translocated across the membrane for the synthesis of an ATP (3), the maximum H^+/e ratio is calculated to be 2.6. This means that the H^+/e ratio of fumarate respiration of *W. succinogenes* should be either 2 or 1, if the H^+/e ratio has to be an integer number. The corresponding values of the ATP/e ratio would be 0.67 and 0.33. To find out whether the higher or the lower ratio is the more likely one, the corresponding percentages relative to the theoretical maximum ratio are compared to those of mitochondrial aerobic respiration with NADH and with succinate. The ATP/e ratios of mitochondrial respiration appear to be well established, and the corresponding percentages are 50 and 57% of the theoretical maximum [44]. The higher (0.67) and the lower (0.33) ATP/e ratio assumed for fumarate respiration amounts to 77% and 38% of the theoretical maximum. The higher ratio is considered to be unlikely, since the ATP gain relative to the theoretical maximum of bacterial respiration is not expected to exceed that of mitochondria by 20% or more. Therefore, the lower ATP/e ratio (0.33) appears to be more likely. Assuming the same percentage as in mitochondrial respiration, the ATP/e ratio of fumarate respiration with H_2 or formate would be close to 0.5, corresponding to a H^+/e ratio of 1.5.

It is generally agreed that the H^+/ATP ratio of ATP synthesis is 4 in mitochondria [1,44]. This number refers to the synthesis of external ATP from external ADP and phosphate. The transport of these compounds is thought to require $1H^+$/ATP. Therefore, the H^+/e ratio is four times the ATP/e ratio in mitochondrial oxidative phosphorylation (Table 2).

NADH is the electron donor in the fumarate respiration of most bacteria forming succinate or propionate under anaerobic conditions [2,45]. The ATP/e ratio of fumarate respiration with NADH has never been determined experimentally. From the reasoning used above, the ratio is predicted to be close to 0.33 (Table 2).

7.2. Determination of the ATP/e ratio

Three different methods have been used for determining the ATP/e ratio of fumarate respiration of *W. succinogenes* (Table 3). In the first method, the ratio was calculated from the extrapolated growth yields (Y^{max}) measured with a chemostat culture. To obtain the ATP gain, Y^{max} was divided by the amount of cells synthesized per mol of ATP (Y^{max}_{ATP}) in the growing culture. Y^{max} was found to vary with the growth conditions. For instance, Y^{max} was considerably

Table 2
Theoretical ATP/e and H^+/e ratios of fumarate respiration compared to those of mitochondrial aerobic respiration

Electron donor	Electron acceptor	$\Delta E'_o$ (V)	ATP/e ratio			H^+/e ratio	
			maximum[a]	assumed	(assumed/maximum) × 100	maximum[b]	assumed
H_2 (HCO_3^-)	Fumarate	0.45	0.87	0.67	77	2.6	2
			0.87	0.33	38	2.6	1
NADH	O_2	1.14	2.2	1.25[c]	57	8.8	5[c]
Succinate	O_2	0.79	1.5	0.75[c]	50	6.0	3[c]
NADH	Fumarate	0.35	0.68	0.33	49	2.0	1

[a] $(n_{ATP}/n_e)_{max}$ calculated according to Eq. 2 with $\Delta G'_P = 50$ kJ/mol ATP and the given values of $\Delta E'_o$.
[b] The values were obtained upon multiplication of $(n_{ATP}/n_e)_{max}$ by 3 (fumarate respiration) or by 4 (aerobic respiration) [1,44].
[c] These values are in agreement with the experimental results [1,44].

Table 3
ATP/e ratios of fumarate respiration

Organism	Method/preparation	Electron donor	ATP/e
W. succinogenes	growth yields	HCO_2^-	0.40 [46]
E. coli	growth yields	H_2	0.22 [47]
W. succinogenes	cells	HCO_2^-	0.45 [43]
W. succinogenes	inverted vesicles	H_2	0.28 [12,48]

higher when the concentration of formate rather than fumarate was growth limiting [46]. When the concentration of fumarate was growth limiting, Y^{max} was 70% the value measured with formate at growth limiting concentration. This can be explained by the finding that *W. succinogenes* uses formate only as a catabolic substrate, whereas fumarate is used in both catabolism and anabolism [49]. Hence Y^{max} and the apparent ATP gain derived from Y^{max} of growing bacteria is higher when the velocity of growth is limited by catabolism and not by anabolism. The Y^{max} used for evaluating the ATP/e ratio of *W. succinogenes* was measured with formate at growth limiting concentration (Table 3). The lower ATP gain obtained for *E. coli* growing with H_2 and fumarate (Reaction a) probably refers to growth limitation by anabolism. The values of Y_{ATP}^{max} used for calculating the ATP gain for the fumarate respiration of *W. succinogenes* (18 g cells mol^{-1} ATP) and of *E. coli* (15.4 g cells/mol ATP) were estimated from the anabolic pathways using several assumptions [46,47].

In the second method, the phosphorylation of the ADP and AMP in cells of *W. succinogenes* was measured as a function of time after initiation of the electron transport from formate to fumarate [43]. The initial velocity of phosphoanhydride formation was divided by the rate of fumarate reduction to obtain the ATP/e ratio (Table 3). The validity of this value is uncertain because phosphorylation and fumarate reduction were measured in different samples of the cell suspension, thus conditions were not quite identical. Furthermore, fumarate reduction was measured photometrically, and the accuracy of this method was impaired by the interference of the variable activity of the fumarase in cells of *W. succinogenes*.

In the third method, inverted membrane vesicles of *W. succinogenes* were used. The formation of 'organic' from inorganic phosphate during fumarate respiration with H_2 was measured in the presence of ADP to determine the ATP/e ratio (Table 3). The fumarate reductase and the ATP synthase of the vesicles were exposed to the outside of the membrane, while hydrogenase and formate dehydrogenase face the inside [18]. This method allowed the measurement of both phosphate esterification in the presence of glucose and hexokinase, and fumarate reduction by H_2 in the same sample. The result so obtained had to be corrected for that proportion of the membrane fraction which catalyzed fumarate reduction, but did not contribute to phosphorylation. This was done by determining the accessibility of formate dehydrogenase to formate, and of fumarate reductase to an external redox dye which does not permeate through the membrane. The activity of formate dehydrogenase was stimulated two-fold upon the addition of a low concentration of a detergent, whereas that of fumarate reductase was not altered. The effect of detergent on the activities indicated that half the preparation consisted of open membrane fragments which perform electron transport without coupled phosphorylation. The other half of the preparation was thought to consist of inverted vesicles catalysing phosphorylation driven by the electron transport. Therefore, the ATP gain given in Table 3 is twice the value actually measured.

A higher value of the ATP/e ratio (0.47) reported earlier with inverted vesicles, was later found to be erroneous [43,50]. This value resulted from plotting the ATP/e ratios as a function of electron transport activity, and extrapolation to zero activity. The electron transport activity was varied by inhibition. Later it was found that the apparent increase in ATP gain with decreasing electron transport activity was due to an artefact [50]. After correction of the experimental data for the artefact, the ATP/e ratio (0.26) was close to that given in Table 3.

Using nearly the same method and the same mem-

brane preparation of *W. succinogenes* catalysing fumarate respiration with H_2, Reddy and Peck [51] measured the ATP/e as 0.1–0.15, and occasionally as high as 0.27. These authors did not correct their values for the non-phosphorylating proportion of their preparation. The lower ATP/e ratios are close to those actually measured by Kröger and Winkler with a preparation, of which half consisted of inverted vesicles (Table 3). The higher value was possibly obtained with a preparation, of which 80% consisted of inverted vesicles. Preparations with 75% inverted vesicles were occasionally obtained from *W. succinogenes* cells [18]. In summary, the ATP/e ratios obtained with inverted vesicles are close to the lower value (0.33) assumed in Table 2, whereas that measured with cells of *W. succinogenes* amounted to 67% of the higher value (0.67). Since the measurements were not sufficiently accurate, the true ATP/e ratio remains to be established. The ATP/e ratios of fumarate respiration with membrane preparations from other bacteria were lower than those obtained with inverted vesicles from *W. succinogenes* [12,52,53].

7.3. Determination of Δp and H^+/e ratios

The electrical proton potential ($\Delta\psi$) generated across the membrane of *W. succinogenes* cells by fumarate respiration with H_2 or formate was determined to be approximately 0.17 V [12,54]. The same value was measured with inverted vesicles catalysing fumarate respiration with H_2. The ΔpH across the membrane of cells generated by the two reactions, and the ΔpH generated across the membrane of inverted vesicles catalysing fumarate respiration with H_2 was found to be negligible. The value of $\Delta p = 0.17$ V is consistent with the chemiosmotic postulates (Eqs. 3 and 4). With $\Delta G'_P = 50$ kJ/mol ATP, the theoretical minimum amount of protons to be translocated for the synthesis of 1 mol ATP $(\nu_{H^+}/n_{ATP})_{min}$ (Eq. 3) is only slightly above the experimentally determined H^+/ATP ratio of 3, indicating that Δp and the cellular phosphorylation potential are close to equilibrium:

$$(\nu_{H^+}/n_{ATP})_{min} = \Delta G'_P/(\Delta pF) \quad (3)$$

$$(n_{H^+}/n_e)_{max} = \Delta E'_o/\Delta p \quad (4)$$

The theoretical maximum H^+/e ratio, $(n_{H^+}/n_e)_{max}$, calculated according to Eq. 4 is 2.6 which would be compatible with an actual H^+/e ratio of 2 or 1 (Table 2).

The H^+/e ratios measured with cells of *W. succinogenes* were below 1, whereas that measured with inverted vesicles was slightly above 1 (Table 4). In contrast, the measured ATP/e ratio is lower than 0.33 in inverted vesicles and higher than 0.33 in cells (Table 3). An H^+/e ratio of 1 corresponds to an ATP/e ratio of 0.33 with H^+/ATP = 3 (see Table 2).

Using a pH electrode the H^+/e ratios given in

Table 4
H^+/e ratios of the electron transport with fumarate or DMN as electron acceptor, and of fumarate reduction by $DMNH_2$

Preparation	Electron donor	Electron acceptor	H^+/e	
Cells	H_2	fumarate	0.75	[55]
Cells	HCO_2^-	fumarate	≤0.8	[56]
Inverted vesicles	H_2	fumarate	1.1	[54]
Proteoliposomes	H_2	fumarate	1.0[a]	
Proteoliposomes	H_2	DMN	0.9[a]	
Proteoliposomes	$DMNH_2$	fumarate	<0.1[a]	[57]
Cells	H_2	DMN	0.6	[57]
Inverted vesicles	H_2	DMN	0.5	[57]

[a]S. Biel and A. Kröger, unpublished results.

The proteoliposomes containing per g phospholipid 10 μmol MK, 20 mg hydrogenase [20], and 180 mg fumarate reductase [38] were prepared with egg yolk phosphatidyl choline [58] as described in [59]. The proteoliposomal suspension was saturated with H_2 (except when $DMNH_2$ was used) and valinomycin was added (0.5 μmol per g phospholipid). Proton release upon the addition of fumarate or DMN was recorded using phenol red and a stopped-flow spectrophotometer. The H^+/e ratio with H_2 and fumarate was calculated from the initial rates of acidification and of fumarate reduction. The values obtained with DMN or $DMNH_2$ were evaluated using the amount of oxidant added.

Table 4 were calculated from the amounts of H^+ released (cells) or taken up (inverted vesicles) upon initiation of electron transport by the addition of small amounts of fumarate. Proton release or uptake was prevented when a protonophore was added before fumarate. The values for cells were measured in the presence of valinomycin (5 μmol/g cell protein) and external K^+ (0.1 M) to minimize the $\Delta\psi$ generated by the electron transport. The H^+/e ratio was not increased by applying higher amounts of valinomycin or by the presence of tetraphenylphosphonium (TPP^+). It is not excluded that the H^+/e ratio measured with cells was lowered by the interference of electrogenic fumarate uptake [60].

The H^+/e ratio measured with valinomycin treated inverted vesicles was a function of the internal concentrations of buffer and K^+. The presence of *N*,*N*′-dicyclohexylcarbodiimide, an inhibitor of the ATP synthase, enhanced the H^+/e value. Under the optimal conditions, the H^+/e ratio slightly exceeded 1 (Table 4). This value was not increased by the addition of SCN^-, which had a considerable effect when valinomycin was absent. This suggests that the $\Delta\psi$ created by fumarate reduction was negligible under these experimental conditions, and did not affect the H^+/e ratio. The internal pH of the vesicles was not significantly altered by fumarate reduction, since the amount of internal buffer exceeded that of fumarate added (and protons taken up) by more than one order of magnitude. The H^+/e ratio (1.1) given in Table 4 was calculated by correcting the experimental value for that proportion of the membrane preparation which performs electron transport without generating a Δp. This correction was done using the procedure applied for correcting the ATP/e ratio measured with the inverted vesicle preparation (see Table 3).

Fumarate reduction by H_2 was found to generate a $\Delta\psi$ of 0.16 V across the membrane of proteoliposomes containing MK, fumarate reductase, and hydrogenase which were isolated form *W. succinogenes* (S. Biel and A. Kröger, unpublished results). The polarity of the $\Delta\psi$ (positive outside) was the same as that measured with cells of *W. succinogenes*. No $\Delta\psi$ was generated in the presence of external K^+, when the proteoliposomes were treated with valinomycin. Under these conditions, the H^+/e ratio of fumarate respiration with H_2 was measured to be 1.0 (Table 4). The H^+/e ratio was zero after treatment of the proteoliposomes with a protonophore. DMN reduction by H_2 (Reaction d) which is known to be catalyzed by hydrogenase:

$$H_2 + DMN \rightarrow DMNH_2 \qquad (d)$$

also generated a $\Delta\psi = 0.16$ V across the membrane of the proteoliposomes. The polarity of the $\Delta\psi$ was the same as that generated by fumarate respiration. The corresponding H^+/e ratio measured in the presence of valinomycin and external K^+ was 0.9. No $\Delta\psi$ was generated in proteoliposomes catalysing fumarate reduction by $DMNH_2$ (Reaction e), and the corresponding H^+/e ratio was negligible. Reaction e is catalyzed by fumarate reductase:

$$DMNH_2 + \text{fumarate} \rightarrow DMN + \text{succinate} \qquad (e)$$

Similar as with the proteoliposomes, Reaction d was found to generate a $\Delta\psi$ in cells and inverted vesicles of *W. succinogenes*, whereas Reaction e did not [57]. The H^+/e ratios (Reaction d) were lower than those observed with the proteoliposomes (Table 4). DMN reduction by formate generated a $\Delta\psi$ in cells of *W. succinogenes* and in proteoliposomes containing formate dehydrogenase [57]. In summary, the Δp generated by fumarate respiration of *W. succinogenes* appears to be exclusively caused by the electron transfer from H_2 (or formate) to MK, whereas the electron transfer from MKH_2 to fumarate apparently does not contribute to Δp generation. This view is confirmed by the nearly equal H^+/e ratios measured for the reduction of DMN and of fumarate by H_2 with the proteoliposomes (Table 4).

Fumarate reductase in the proteoliposomes was fully accessible to external fumarate (S. Biel and A. Kröger, unpublished results). This indicates that all the fumarate reductase molecules face the outside. The orientation of hydrogenase which cannot be measured accurately, is probably the same as that of fumarate reductase. The orientation of the hydrogenase molecules within the liposomal membrane is expected to have a critical effect on the H^+/e ratio value. The measured H^+/e ratio would be lower, if some of the hydrogenase molecules faced the inside (see Fig. 4). Therefore, it cannot be excluded that the true H^+/e ratio is higher than 1.

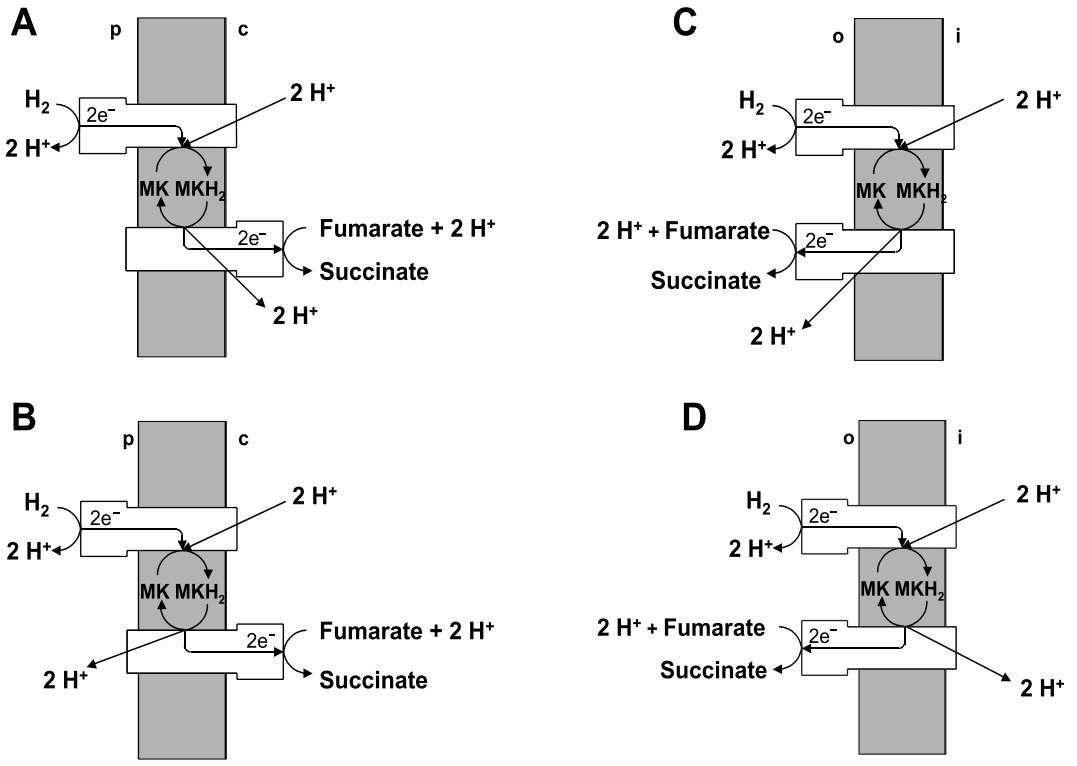

Fig. 4. Hypothetical mechanisms of Δp generation by fumarate respiration with H_2. (A) and (B) refer to the membrane of *W. succinogenes* (p, periplasmic side; c, cytoplasmic side). (C) and (D) refer to the proteoliposomes (o, outside; i, inside) (Table 4). Equivalent mechanisms are thought to apply with formate as electron donor.

8. Mechanism of Δp generation

The substrate site of hydrogenase (and of formate dehydrogenase) in *W. succinogenes* cells is exposed to the periplasmic side of the membrane [17] (Fig. 4A,B). Therefore, the oxidation of H_2 at the substrate site of hydrogenase is likely to result in the release of 2 H^+ on the periplasmic side of the membrane (Section 3). The protons simultaneously consumed in MK reduction are thought to be taken up from the cytoplasmic side of the membrane. This assumption is based on the finding that quinone reduction by H_2 causes Δp generation across the membrane and that the H^+/e ratio of this process is close to 1 (Table 4). However, it is not excluded that the protons are taken up from the periplasmic side and that hydrogenase operates as a proton pump with a H^+/e ratio of 1. The substrate site of fumarate reductase is exposed to the cytoplasmic side of the membrane [18]. Therefore, the reduction of fumarate at the substrate site is associated with the uptake of 2 H^+ from the cytoplasmic side. The protons formed on MKH_2 oxidation by fumarate reductase are thought to be released on the cytoplasmic side (Fig. 4A). This conclusion is based on the observation that quinol oxidation by fumarate is not associated with membrane polarization or apparent proton translocation (Table 4). The electroneutrality of quinol oxidation by fumarate is confirmed by the finding that the same H^+/e ratio of nearly 1 is observed in H_2 oxidation by quinone and by fumarate with the proteoliposomes, in agreement with Fig. 4C. Furthermore, the H^+/e ratio of H_2 oxidation by fumarate was found to be independent of the relative orientations of fumarate reductase and hydrogenase in the membrane (Fig. 4A,C). About the same H^+/e ratio was measured with cells and with inverted vesicles with opposite orientation of the two enzymes, as well as with proteoliposomes containing the enzymes in the same orientation (Table 4). In contrast, the H^+/e should be 2 with cells and inverted vesicles (Fig. 4B), and 0 with liposomes (Fig. 4D), if fumarate reductase was electrogenic. Thus the mechanism of fumarate respiration shown in Fig. 4A which pos-

tulates the H^+/e ratio to be 1, is more consistent with the experimental results than that shown in Fig. 4B which predicts a H^+/e ratio of 2.

If menaquinol oxidation by fumarate was coupled to Δp generation in *W. succinogenes*, the actual H^+/e ratio should be well below 1. According to Eq. 4 with $\Delta p = 0.17$ V and the redox potentials of MK/MKH_2 ($E'_o = -75$ mV, in organic solution) and of fumarate/succinate ($E'_o = +30$ mV), $(n_{H^+}/n_e)_{max}$ is calculated to be 0.6. For a value of $(n_{H^+}/n_e)_{max}$ exceeding 1, the actual redox potential of MK/MKH_2 in the membrane would have to be more than 65 mV lower than E'_o in organic solution. The ratio MK/MKH_2 in the membrane fraction catalysing fumarate reduction by formate is not far from 1, and the value of E'_o of MK/MKH_2 in the membrane is expected to be close to that in organic solution [36,61].

9. The site of menaquinol oxidation in fumarate reductase

The experimental results discussed above suggest that the oxidation of MKH_2 by fumarate, which is catalyzed by the fumarate reductase of *W. succinogenes*, is an electroneutral process. The protons formed by MKH_2 oxidation are assumed to be released to the cytoplasmic side of the membrane where they balance the protons consumed by fumarate reduction (Fig. 4A). However, the site of MKH_2 oxidation on the cytochrome *b* subunit (FrdC) of fumarate reductase is not known and no specific inhibitor of MKH_2 oxidation has been identified. In the crystal structure, a cavity which extends from the hydrophobic phase of the membrane, close to the distal heme group of FrdC, to the periplasmic aqueous phase could accommodate a MKH_2 molecule, after minor structural alterations [62]. A glutamate residue (E-66) lines the cavity and could accept a hydrogen bond from one of the hydroxyl groups of MKH_2 (Fig. 3). Replacement of E-66 by a glutamine residue resulted in a mutant (E66Q) which did not catalyze $DMNH_2$ oxidation by fumarate, whereas the activity of fumarate reduction by benzylviologen radical was not affected by the mutation [62]. X-ray crystal structure analysis of the E66Q variant enzyme ruled out significant structural alterations. No significant reduction of the high-potential heme by $DMNH_2$ was possible, although the midpoint potentials of the two heme groups were virtually unaffected. These results indicate that the inhibition of quinol oxidation activity in the mutant enzyme is due to absence of the carboxyl group of E-66. In the wild-type enzyme, E-66, which is conserved in the fumarate reductase enzymes from the ε-proteobacteria *Campylobacter jejuni* and *Helicobacter pylori* (see Lancaster and Simon, this volume) and is an aspartate in *B. subtilis* succinate dehydrogenase [63], seems to serve as the direct acceptor of one of the protons formed by quinol oxidation; since there is no structural indication of a proton channel within FrdC which would guide the protons formed in MKH_2 oxidation to the cytoplasmic side of the membrane, the protons are expected to be released into the periplasm via the cavity as depicted schematically in Fig. 4B. This would mean that quinol oxidation by fumarate is an electrogenic process in *W. succinogenes* with an H^+/e ratio of 1. However, this prediction has not been confirmed experimentally.

10. Mechanism of succinate oxidation in *B. subtilis*

B. subtilis succinate dehydrogenase is predicted to be structurally similar to *W. succinogenes* fumarate reductase [13]. This includes the cytochrome *b* subunits, which share considerable sequence similarity [63]. The two heme groups in SdhC of succinate dehydrogenase are probably arranged in the same way as in FrdC of *W. succinogenes* (Fig. 3). The proximal heme group is predicted to be close to the trinuclear iron–sulfur center on the cytoplasmic side of the membrane, and the distal heme close to the periplasmic membrane surface. The distance between the heme groups should allow rapid electron transfer.

The two enzymes catalyze succinate oxidation by quinones and fumarate reduction by quinols at commensurate turnover numbers; they react with naphthoquinones as well as with benzoquinones (Section 5.1). The two enzymes differ in their sensitivity to HQNO [33]. The reduction of Q_O by succinate as well as fumarate reduction by $DMNH_2$ catalyzed by succinate dehydrogenase, were inhibited by NQNO. The oxidation of succinate by PMS/DCPIP was not inhibited. Fumarate reductase is insensitive to HQNO, both in succinate oxidation with quinones

and in the reverse reaction. HQNO appears to be bound to the low-potential heme of succinate dehydrogenase, whose midpoint potential is shifted to a more electro-negative value in the presence of HQNO [64]. The properties of *B. subtilis* mutants with substitution of a histidyl residue coordinating the distal heme suggest that the distal heme is the low-potential one and that the distal heme group is close to the site of quinone reduction [65]. This is consistent with the view that HQNO interacts at the quinone site. Thus the site of quinone reduction appears to be near the distal heme of succinate dehydrogenase SdhC.

The physiological role of *B. subtilis* succinate dehydrogenase differs from that of a fumarate reductase. Succinate dehydrogenase serves as a constituent of the citrate cycle and of the respiratory chain in the obligately aerobic *B. subtilis* [13]. The *B. subtilis* enzyme catalyzes the oxidation of succinate by MK (Reaction f), an endergonic reaction:

$$\text{succinate} + \text{MK} \underset{\Delta G'_o = +20\ \text{kJ/mol}}{\longrightarrow} \text{fumarate} + \text{MKH}_2 \quad \text{(f)}$$

The respiratory activity of *B. subtilis* cells with succinate was found to be nearly abolished by the presence of a protonophore [66,67]. This suggests that the endergonic reaction (Reaction f) is driven by the Δp generated by the MKH_2 oxidation with O_2 in the absence of the protonophore. The hypothetical coupling mechanism is depicted in Fig. 5A. Reaction f is coupled to the uptake of $2H^+$ from the outside and the release of $2H^+$ on the cytoplasmic side of the membrane. At a $\Delta p = 0.17$ V, the apparent proton translocation driving Reaction f provides a ΔG of -33 kJ, so that the overall reaction (Reaction g) would be exergonic with a ΔG of -13 kJ/mol succinate oxidized, assuming equal concentrations of succinate and fumarate and of MK and MKH_2. H_o^+ and H_i^+ in Reaction g designate protons on the outside and the inside of the membrane, respectively:

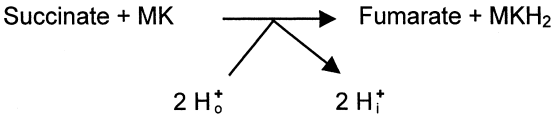

(g)

Thus, the hypothetical mechanism (Fig. 5A) is energetically feasible, and may explain the inhibition of the activity of succinate respiration by protonophores in *B. subtilis* cells.

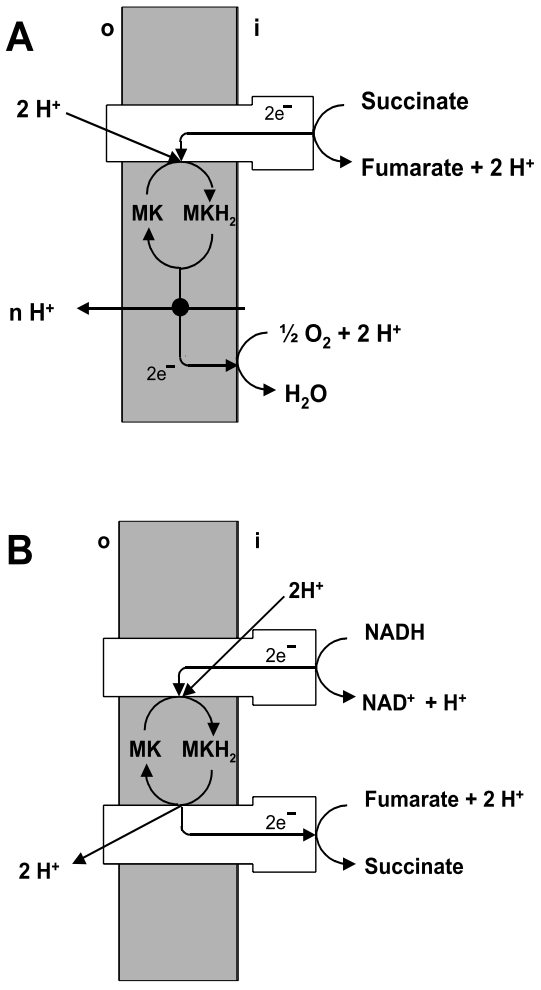

Fig. 5. Hypothetical mechanisms of succinate oxidation by MK (A) and of fumarate reduction by NADH (B) in the membrane of *B. subtilis* (o, outside; i, inside). The number of protons apparently translocated by MKH_2 oxidation with O_2 (u H^+) includes the protons released by MKH_2 oxidation (A).

The view that succinate oxidation by MK is driven by Δp (Fig. 5A) is confirmed by the finding that fumarate reduction by NADH is coupled to Δp generation in *B. subtilis* cells (Fig. 5B) [67]. It can be seen from the genome that *B. subtilis* has only one NADH dehydrogenase which is similar to the non-coupling Ndh enzyme of *E. coli*. Therefore, NADH oxidation by MK is not expected to contribute to Δp generation in *B. subtilis* respiration. Using a mutant lacking a functional succinate dehydrogenase, it was shown that this enzyme is involved in the electron transport from NADH to fumarate. In a similar

way, MK was shown to be a constituent of the electron transport chain. As expected, fumarate reduction by NADH was not inhibited by protonophores, in contrast to succinate respiration. As depicted in Fig. 5B, the oxidation of MKH_2 by fumarate catalyzed by succinate dehydrogenase is thought to be electrogenic, and to be responsible for Δp generation by fumarate reduction with NADH. Thus the Δp is generated by the reversal of Reaction g, which explains why succinate oxidation is driven by Δp in *B. subtilis*. The H^+/e ratio of 1 predicted by Fig. 5B and Reaction g, has not yet been confirmed experimentally. In summary, the succinate dehydrogenase of *B. subtilis* appears to be electrogenic, in contrast to the apparent electroneutrality of *W. succinogenes* fumarate reductase.

Acknowledgements

This work was supported by grants of the Deutsche Forschungsgemeinschaft and by the Fonds der Chemischen Industrie to A.K. and G.U.

References

[1] D.G. Nicholls, S.J. Ferguson, Bioenergetics 2, Academic Press, London, 1992.
[2] G. Unden, J. Bongaerts, Biochim. Biophys. Acta 1320 (1997) 217–234.
[3] B. Berks, S.J. Ferguson, J.W.B. Moir, D.J. Richardson, Biochim. Biophys. Acta 1232 (1995) 97–173.
[4] R. Hedderich, O. Klimmek, A. Kröger, R. Dirmeier, M. Keller, K.O. Stetter, FEMS Microbiol. Rev. 22 (1999) 353–381.
[5] H. Michel, Biochemistry 38 (1999) 15129–15140.
[6] A.R. Crofts, S. Hong, N. Ugulava, B. Barquera, R. Gennis, M. Guernova-Kuras, E.A. Berry, Proc. Natl. Acad. Sci. USA 96 (1999) 10021–10026.
[7] S. Iwata, C. Ostermeier, B. Ludwig, H. Michel, Nature 376 (1995) 660–669.
[8] C.R.D. Lancaster, A. Kröger, M. Auer, H. Michel, Nature 402 (1999) 377–385.
[9] T. Ohnishi, C.C. Moser, C.C. Page, P.L. Dutton, T. Yano, Structure 8 (2000) R23–R32.
[10] L. Hederstedt, T. Ohnishi, in: L. Ernster (Ed.), Molecular Mechanisms Bioenergetics, Elsevier Science, Amsterdam, 1992, pp. 163–198.
[11] B.A.C. Ackrell, M.K. Johnson, R.P. Gunsalus, G. Cecchini, in: F. Müller (Ed.), Chemistry and Biochemistry of Flavoenzymes, CRC Press, Boca Raton, FL, 1992, pp. 229–284.
[12] A. Kröger, V. Geisler, E. Lemma, F. Theis, R. Lenger, Arch. Microbiol. 185 (1992) 311–314.
[13] C. Hägerhäll, Biochim. Biophys. Acta 1320 (1997) 107–141.
[14] C.R.D. Lancaster, A. Kröger, Biochim. Biophys. Acta 1459 (2000) 422–431.
[15] J. Simon, R. Gross, O. Klimmek, A. Kröger, in: M. Dworkin et al. (Eds.), The Prokaryotes: an Evolving Electronic Resource for the Microbiological Community, 3rd edn., Springer, Berlin, 2000.
[16] B.C. Berks, M.D. Page, D.J. Richardson, A. Reilly, A. Cavill, F. Outen, S.J. Ferguson, Mol. Microbiol. 15 (1995) 319–331.
[17] R. Groß, J. Simon, F. Theis, A. Kröger, Arch. Microbiol. 170 (1998) 50–58.
[18] A. Kröger, E. Dorrer, E. Winkler, Biochim. Biophys. Acta 589 (1980) 118–136.
[19] J. Simon, R. Gross, M. Ringel, E. Schmidt, A. Kröger, Eur. J. Biochem. 251 (1998) 418–426.
[20] F. Droß, V. Geisler, R. Lenger, F. Theis, T. Krafft, F. Fahrenholz, E. Kojro, A. Duchêne, D. Tripier, K. Juvenal, A. Kröger, Eur. J. Biochem. 206 (1992) 93–102.
[21] R. Groß, J. Simon, C.R.D. Lancaster, A. Kröger, Mol. Microbiol. 30 (1998) 639–646.
[22] A. Volbeda, M.-H. Charon, C. Piras, E.C. Hatchikian, M. Frey, J.C. Fontecilla-Camps, Nature 373 (1995) 580–587.
[23] Y. Higuchi, T. Yagi, N. Yasuoka, Structure 5 (1997) 1671–1680.
[24] R. Lenger, U. Herrmann, R. Gross, J. Simon, A. Kröger, Eur. J. Biochem. 246 (1997) 646–651.
[25] M. Bokranz, M. Gutmann, C. Körtner, E. Kojro, F. Fahrenholz, F. Lauterbach, A. Kröger, Arch. Microbiol. 156 (1991) 119–128.
[26] M.-A. Mandrand-Berthelot, G. Couchoux-Luthaud, C.-L. Santini, G. Giordano, J. Gen. Microbiol. 134 (1988) 3129–3139.
[27] G. Unden, A. Kröger, Biochim. Biophys. Acta 682 (1982) 258–263.
[28] G. Unden, A. Kröger, Biochim. Biophys. Acta 725 (1983) 325–331.
[29] A. Jankielewicz, R.A. Schmitz, O. Klimmek, A. Kröger, Arch. Microbiol. 162 (1994) 238–242.
[30] J.C. Boyington, V.N. Gladyshev, S.V. Khangulov, T.C. Stadtman, P.D. Sun, Science 275 (1997) 1305–1308.
[31] G. Unden, H. Hackenberg, A. Kröger, Biochim. Biophys. Acta 591 (1980) 275–288.
[32] G. Unden, A. Kröger, Eur. J. Biochem. 120 (1981) 577–584.
[33] E. Lemma, C. Hägerhäll, V. Geisler, U. Brandt, G. von Jagow, A. Kröger, Biochim. Biophys. Acta 1059 (1991) 281–285.
[34] G. Unden, S.P.J. Albracht, A. Kröger, Biochim. Biophys. Acta 767 (1984) 460–469.
[35] C.C. Page, C.C. Moser, X. Chen, P.L. Dutton, Nature 402 (1999) 47–52.

[36] A. Kröger, A. Innerhofer, Eur. J. Biochem. 69 (1976) 487–495.
[37] G. Unden, E. Mörschel, M. Bokranz, A. Kröger, Biochim. Biophys. Acta 725 (1983) 41–48.
[38] G. Unden, A. Kröger, Methods Enzymol. 126 (1986) 387–399.
[39] M. Graf, M. Bokranz, R. Böcher, P. Friedl, A. Kröger, FEBS Lett. 184 (1985) 100–103.
[40] A. Kröger, E. Winkler, A. Innerhofer, H. Hackenberg, H. Schägger, Eur. J. Biochem. 94 (1979) 465–475.
[41] M. Bokranz, E. Mörschel, A. Kröger, Biochim. Biophys. Acta 810 (1985) 332–339.
[42] A. Brune, J. Spillecke, A. Kröger, Biochim. Biophys. Acta 893 (1987) 499–507.
[43] A. Kröger, E. Winkler, Arch. Microbiol. 129 (1981) 100–104.
[44] P.C. Hinkle, M.A. Kumar, A. Resetar, D.L. Harris, Biochemistry 30 (1991) 3576–3582.
[45] A. Kröger, in: B.A. Haddock, W.A. Hamilton (Eds.), Microbial Energetics, Cambridge University Press, Cambridge, 1977, pp. 61–93.
[46] H. Mell, M. Bronder, A. Kröger, Arch. Microbiol. 131 (1982) 224–228.
[47] T. Bernhard, G. Gottschalk, Arch. Microbiol. 116 (1978) 235–238.
[48] M. Bokranz, J. Katz, I. Schröder, A.M. Roberton, A. Kröger, Arch. Microbiol. 135 (1983) 36–41.
[49] M. Bronder, H. Mell, E. Stupperich, A. Kröger, Arch. Microbiol. 131 (1982) 216–223.
[50] C. Wellnitz, Diploma thesis, University of Marburg, FB Biologie, 1985.
[51] C.A. Reddy, H.D. Peck Jr., J. Bacteriol. 134 (1978) 982–991.
[52] L.L. Barton, J. LeGall, H.D. Peck, Biochem. Biophys. Res. Commun. 41 (1970) 1036–1042.
[53] K. Miki, E.C.C. Lin, J. Bacteriol. 124 (1975) 1282–1287.
[54] H. Mell, C. Wellnitz, A. Kröger, Biochim. Biophys. Acta 852 (1986) 212–221.
[55] H. Mell (1985), Doctoral thesis, University of Marburg, FB Biologie.
[56] A. Kröger, Biochim. Biophys. Acta 505 (1978) 129–145.
[57] V. Geisler, R. Ullmann, A. Kröger, Biochim. Biophys. Acta 1184 (1994) 219–226.
[58] W.S. Singleton, M.S. Gray, M.L. Brown, J.L. White, J. Am. Oil Chem. Soc. 42 (1965) 53–56.
[59] O. Lambert, D. Levy, J.-L. Ranck, G. Leblanc, J.-L. Rigaud, Biophys. J. 74 (1998) 918–930.
[60] R. Ullmann, R. Gross, J. Simon, G. Unden, A. Kröger, J. Bacteriol. 182 (2000) 5757–5764.
[61] U. Liebl, S. Pezennec, A. Riedel, E. Kellner, W. Nitschke, J. Biol. Chem. 267 (1992) 14068–14072.
[62] C.R.D. Lancaster, R. Gross, A. Haas, M. Ritter, W. Mäntele, J. Simon, A. Kröger, Proc. Natl. Acad. Sci. USA 97 (2000) 13051–13056.
[63] C. Hägerhäll, L. Hederstedt, FEBS Lett. 389 (1996) 25–31.
[64] I.A. Smirnova, C. Hägerhäll, A.A. Konstantinov, L. Hederstedt, FEBS Lett. 359 (1995) 23–26.
[65] M. Matsson, R. Tolstoy, R. Aasa, L. Hederstedt, Biochemistry 39 (2000) 8617–8624.
[66] J. Schirawski, G. Unden, Eur. J. Biochem. 257 (1998) 210–215.
[67] M. Schnorpfeil, I.G. Janausch, S. Biel, A. Kröger, G. Unden, Eur. J. Biochem. 268 (2001) 3069–3074.